Tellus (1998), 50B, 353–365
Printed in UK – all rights reserved

TELLUS
ISSN 0280–6509

Carbon monoxide fluxes of different soil layers in upland Canadian boreal forests

By THOMAS A. J. KUHLBUSCH[1,*‡], R. G. ZEPP[2], W. L. MILLER[1,#] and R. A. BURKE, Jr.[2]
[1]*National Research Council, c/o U. S. Environmental Protection Agency, Athens, GA 30605, USA,*
[2]*Ecosystem Research Division, National Exposure Research Laboratory, US Environmental Protection Agency, Athens, GA 30605, USA*

(Manuscript received 14 April 1997, in final form 11 March 1998)

ABSTRACT

Dark or low-light carbon monoxide fluxes at upland Canadian boreal forest sites were measured on-site with static chambers and with a laboratory incubation technique using cores from different depths at the same sites. Three different upland black spruce sites, burned in 1987, 1992 and 1995 and a control site, were chosen to determine the effects of fire, temperature, soil structure and soil covers on CO fluxes. Three different surfaces were observed at the sites — bare mineral soil with little living moss cover; burned feather mosses 5–30 cm deep; and unburned, living, green feather mosses. The static chamber measurements indicated similar deposition velocities for the burned and unburned feather moss sites [$(1.54 \pm 0.64) \cdot 10^{-2}$ cm s^{-1}; $(1.83 \pm 0.63) \cdot 10^{-2}$ cm s^{-1}], but significantly lower rates for sites that had burned down to the mineral soil [$(1.08 \pm 0.53) \cdot 10^{-2}$ cm s^{-1}, excluding data with net CO emission]. This finding was confirmed by results from the incubation measurements and shows that fire intensities determine the long-term, post-fire effect on soil-atmosphere fluxes of CO. Temperature studies with the cores showed that CO consumption rates increased from (2 ± 1)% at -15°C to -13°C to (43 ± 20)% at 0°C to 1.5°C and (68 ± 15)% at 4°C to 5°C of the deposition velocity values obtained at 20°C. This temperature dependence was consistent with results obtained from the static chamber measurements. The temperature range studied and the dark or low-light conditions were representative for the night-time of nearly the whole six snow-free months in the boreal ecosystem. In nearly all cases, deposition velocities determined for cores from the top 5 cm with the incubation technique were the same, within experimental errors, as those determined with the static chambers. Soil CO concentration profiles taken in situ, moreover, did not show any clear trend below 5 cm. Thus we conclude that the top 5 cm of soils are determining the dark soil-atmosphere CO fluxes at these sites. The top 5 cm of soil columns are most exposed to temperature (and probably moisture) variations and are most affected by fires as well.

1. Introduction

Carbon monoxide (CO) is one of the main atmospheric trace gases controlling the distribution of ozone (O_3) and hydroxyl radicals (OH), the dominant oxidising species in the troposphere. In balancing the global CO cycle, soils may act as sources or sinks. CO is known to be produced in soils thermally (Conrad and Seiler, 1985a) and photochemically (Wilks, 1959; Troxler, 1972; Tarr et al., 1995) from organic matter. Microbial processes are responsible for the oxidation of CO and thus give soils the capacity to act as a sink. Therefore the net soil-atmosphere flux of CO is a result of these physical, chemical, and microbial

‡ Corresponding author
* Current and corresponding address: University of Duisburg, Aerosol and Process Measurement Techniques, Bismarckstr. 81, 47057 Duisburg, Germany. e-mail: tky@uni-duisburg.de
# Current address: Dept. of Oceanography, Dalhousie University Halifax, Nova Scotia, Canada B3H 4J1

processes, acting simultaneously. The global CO sink of soils has been estimated to range from 190–580 Tg yr^{-1}, which is equivalent to approximately 15% of the total annual production of CO (Conrad, 1995). Conrad and Seiler (1985b) showed that CO deposition velocities were nearly independent of temperature between 20°C and 46°C, but that a strong correlation exists between thermally produced CO and soil temperature. They concluded that, for a given system, the temperature controls whether soils act as a sink or a source.

So far, most studies determining soil-atmospheric CO fluxes have been in temperate, subtropical or tropical regions. Net dark CO fluxes in a dry tropical savanna during the rainy season ranged from -1.0 to $+2.0 \cdot 10^{11}$ molecules cm^{-2} s^{-1} (positive values denote soil emissions of CO, ambient CO 220–280 ppb) with a diel average of $0.056 \cdot 10^{11}$ molec. cm^{-2} s^{-1} (Scharffe et al., 1990). Fluxes determined in a nearby semidecidous forest showed a clear net consumption of CO of $-2.4 \cdot 10^{11}$ molec. cm^{-2} s^{-1} at soil surface temperatures of 27°C. CO fluxes determined in a temperate forest near Mainz, Germany, gave net fluxes of -0.24 to $-4.00 \cdot 10^{11}$ molec. cm^{-2} s^{-1} (Conrad and Seiler, 1980).

Only one study reporting soil-atmosphere CO fluxes in boreal forests has been conducted to our knowledge (Zepp et al., 1998) even though this northern zone represents one of the Earth's largest biomes (Kasischke et al., 1995). Using transparent chamber tops, this study found net CO fluxes of undisturbed, upland black spruce and jack pine stands ranging from 0.00 to $-1.30 \cdot 10^{11}$ molec. cm^{-2} s^{-1}, depending mainly on temperature and incident light. The same measurements conducted at recently burned sites showed that fire converted the area from a sink to a source during the summer (Zepp et al., 1998). Whether this change from sink to source is due to increases in the sources or decreases in the sink activity is unknown. The source strength after a fire may increase due to the removal of the tree cover and the resultant higher incident light levels and soil temperatures. Soil warming is further reinforced through more efficient light absorption by blackened, charred surface material that remains for years after a boreal forest fire. Light-induced CO formation from this blackened, charred material may be higher due to enhanced absorbance as well. Sink activity by these soils after a fire may be lower due to the destruction of the microbial substrate. The location of maximal CO consumption in soil columns, e.g., the LFH (Litter, Fibric, Humus) or upper mineral soil layer, is unknown but important for an assessment of the impact of fires, climate change, and changes during succession on soil-atmosphere CO fluxes.

This study was conducted to address the above questions related to fire impact and to quantify net CO fluxes in the dark for different soil layers from boreal black spruce stands at temperatures ranging from -15°C to 20°C.

2. Study sites and experimental

2.1. Site description

Sites chosen for this study have been described in detail elsewhere (Zepp et al., 1998). Briefly, four black spruce sites (56°09′ N, 96°44′ W) were selected about 100 km north of Thompson, Manitoba, Canada. The soil of all sites can be characterised as highly calcareous lacustrine clay in an area of moderate relief (Beke et al., 1973). The control site (CBS) has not burned for at least 80 years whereas the other three sites were exposed to major fires in 1987 (87BS), 1992 (92BS), and 1995 (95BS). The fire regime at all three sites can be classified as intense surface and crown fires (Van Wagner, 1983). Moisture is one factor influencing the intensity of surface fires and thus determining whether surface organic layers get completely burned exposing the top of the mineral soil (Bessie and Johnson, 1995).

The forest floor of the control site was predominantly covered with a thick layer of feather mosses, mainly *Pleurozium schreberii* and *Hylocomium splendens*. Two distinctly different forest floor covers at the burned sites were observed and studied — areas that were burned down to the mineral soil and areas where 5–30 cm of the original organic matter remained on the surface. In the former, only ash and some charred material was on top of the mineral soil, and during succession, a fire-dependent moss (*Ceratodon purpureas*) had started to grow. In the other areas, the F- and H-layers of the original soil cover (feather mosses) were still identifiable with only the surface being charred by the fire.

2.2. CO flux chambers and jar experiments

Soil-atmosphere CO exchange was measured at these sites using transparent, static soil chambers. All studies reported here were conducted in the dark (chamber covered) or under low-light conditions (total solar irradiance $\leqslant 100\ W\ m^{-2}$). The chambers consisted of two parts: a round, semi-permanent aluminium base installed into the ground at least one year prior to the measurements and a removable borosilicate glass cover (~ 24 cm i.d., 25 cm deep) that isolated the atmosphere immediately above the base. The chamber was hermetically sealed by placing the cover into a water-filled trough attached to the top of the base. Two holes drilled into the sides of the glass cover were plugged with small corks. Needles were inserted through the corks to serve as sampling and vent ports. 20-ml gas samples were collected in gas-tight glass syringes sealed with a small amount of water directly after placing the glass cover onto the base and every 7 min until 21 min thereafter. For further details see Zepp et al. (1998).

Samples of the different soil layers were collected in the vicinity of the chamber bases. Small pits were dug and plastic rings (PVC, 5.2 cm i.d., 6.0 cm o.d., 5 cm high) were carefully inserted from the top into the soils. A sharp knife was used to cut any roots or debris to avoid compaction as much as possible. After the insertion of the plastic ring a spatula was used to close off the bottom. Then the ring was cleaned from the outside and put into a sealed glass jar (Ball jar, 500 ml, Alltristo Corp., Muncie, Indiana). Sample ports were drilled into the lids and sealed with carbon-free silicone. The jars were stored at around 0°C in a cooler and transported to our field laboratory. There the samples were stored in a freezer at −15°C until the first measurements were conducted, about 15–20 h after sampling. Intact, whole-core samples were used to minimise physical disturbances of the soil structure which would alter diffusivity and possibly reaction rates (Alperin and Reeburgh, 1985). The bulk dry density data and visual observations of the moss, F-, and H-layers show the high porosity and indicate that the diffusion of gases (e.g., oxygen, CO) throughout these layers is rapid. Thus at least for these layers perturbation of soil condition (aeration) can be neglected. Because only the soil surface of the cores was in contact with the jar air, core measurements were physically equivalent to the static chamber measurements in the field.

Blank measurements of the jars including the plastic ring were conducted since plastic material is known to thermally produce CO. Blank CO deposition velocities of $-0.006 \cdot 10^{-2}\ cm\ s^{-1}$, $-0.030 \cdot 10^{-2}\ cm\ s^{-1}$, $-0.039 \cdot 10^{-2}\ cm\ s^{-1}$, and $-0.06 \cdot 10^{-2}\ cm\ s^{-1}$ were determined for 5°C, 10–15°C, 15–20°C, and 30°C, respectively. These values lie within the range of experimental error and represent in general only 1–4% of the measured deposition velocity but in the opposite direction. We did not correct the determined values for this insignificant error.

Prior to the measurement of CO fluxes, the jars were opened for 15–20 min. to allow the jars to completely fill with laboratory air (200–400 ppb CO). Two different techniques were used to determine net CO deposition fluxes in the jars. In the beginning, 10 ml of standard air (481 ppb CO) was added to the jar head space using a gas-tight syringe and a needle inserted through the silicone port. The syringe was flushed three times and then 10 ml of the air in the jar was sampled. This procedure was repeated 5 times within a time period adjusted to the deposition fluxes, not exceeding 20 min. This technique was used to confirm that the CO deposition flux can be described by a first order rate expression. After that was confirmed for the whole temperature (−15°C to +20°C) and concentration range (500 to 50 ppb), samples were only taken at the start and an appropriate time at the end of each run. The initial sample was taken with the procedure explained above, whereas the final sample was withdrawn from the jar after flushing without addition of standard air. At each temperature and with each sample, 2 to 4 runs were measured. The end time of each run was varied significantly around the half life of CO, if possible.

Prior to the measurement of CO fluxes, the jars were equilibrated at the temperature of the study for at least 12 h. Temperatures were regulated by a deep freezer (−13°C to −15°C), ice water in a cooler (0°C), or a refrigerator (3–5°C). For studies near 20°C, the jars were allowed to adjust to room temperature. Control studies showed that 12 h were enough time for the samples to adjust to the temperature of the surrounding medium (air or water).

Vertical profiles of CO concentrations in air in the moss layers at the various sites were measured to determine concentration gradients and in situ equilibrium CO concentrations if no gradient was detectable. Stainless steel tubes (30 cm long, 2 mm i.d.) directly connected to a gas-tight glass syringe were inserted vertically or horizontally (after digging a pit) into the moss at the desired depth, tube and the syringe flushed using a three-way valve, and then further inserted at the desired depth. The entrapped moss air (20–30 ml) was sampled for subsequent CO analysis.

2.3. CO measurements and auxiliary data

Analysis of samples was conducted as soon after collection as possible, generally within 5 to 6 h for field samples and 5 to 10 min for jar samples. Field-collected syringe samples were stored on ice and in the dark during transport to the laboratory. Previous examination of samples treated in this manner showed changes in CO of less than 2% over a 20-hour period. Carbon monoxide concentrations were measured with a Trace Analytical (Menlo Park, CA, U. S. A.) RGA-3 Reduction Gas Analyser, which was calibrated each day with a standard (481 ± 3 ppb, Scott Marin, further details in Zepp et al., 1998). Deposition velocities for CO sink activity were derived from linear regression analysis of the natural logarithms of CO concentrations versus time. For CO source activity, a linear regression analysis of CO concentrations versus time was performed. The resulting slope was then multiplied by the volume of the chamber or jar and divided by the surface area of the sample to derive deposition velocities in cm s^{-1}.

In addition to CO exchange, data on air and soil temperature, solar irradiance (field measurements), soil moisture, and density were collected. Soil temperature was measured at the depth indicated referenced to the upper surface of the forest floor, regardless of its composition. Gravimetric soil moisture from soil cores (upper 5 cm of the mineral soil) sampled on the same day as the CO measurement was measured by weight loss after 24 h at 80°C and expressed as weight percent water on a dry matter basis. Similarly, soil moisture and bulk density were determined directly from the soil and plant material used in the jar studies.

3. Results

3.1. Static chamber measurements

Generally three different types of soil covers at the study sites can be differentiated: green living moss (feather mosses, *Pleurozium schreberii* and *Hylocomium splendens*), burned feather moss with the top layer being charred, and sites that were burned down to the mineral clay layer. The latter had some new fire-dependent moss (*Ceratodon purpureas*) growing on a charcoal and ash layer. This charcoal and ash layer on top of the mineral clay was still identifiable in a soil pit at the CBS site that had not burned during the last 80 years.

Ambient CO concentration during the static chamber CO measurements ranged between 80 ppb and 170 ppb. Table 1 summarises the results of static chamber CO measurements under dark or low-light conditions to exclude/minimise light-induced CO formation. CO deposition velocities beside fluxes are reported. Only CO deposition velocities are used for the discussion since they are independent from ambient CO concentrations (in contrast to CO fluxes). Deposition velocities can be converted to fluxes by multiplication with ambient CO concentrations. Grouping the deposition fluxes by soil surface type gives average values of $(1.08 \pm 0.53) \cdot 10^{-2}$ cm s^{-1}, $(1.54 \pm 0.64) \cdot 10^{-2}$ cm s^{-1}, and $(1.83 \pm 0.63) \cdot 10^{-2}$ cm s^{-1} for new, burned, and green moss, respectively (Table 2, excluding net CO emissions). These values show a significant difference (*t*-test: $P > 95\%$) between areas that were burned down to the mineral soil and areas where only the top few centimetres of the moss cover was burned. A slight decrease in the CO sink activity is indicated by a lower average deposition velocity for the burned moss as compared to the green, living feather mosses, although this difference is not significant.

Fig. 1 and Table 2 show the temperature dependence of dark deposition velocities determined with the static chambers.

3.2. Incubation measurements

17 soil cores from various depths at these sites were collected in October 1996 and three in September 1995 to determine the vertical distribution of CO consumption. No auxiliary data were

Table 1. *Static chamber CO deposition fluxes under dark or low light conditions*

Site	Surface	Date	Dep. Vel. [10^{-2} cm/s]	Flux [10^{9} molec/s/cm^2]	R^2	Light [W m^{-2}]	Moisture [%-dm]	Sur. Temp. [°C]
87BS-A	*Ceratodon*	29-May-96	0.86±0.09	−31.2±2.5	0.966	0	n.d.	24.4
87BS-A	*Ceratodon*	4-Jun-96	1.94±0.39	−51.3±13.5	0.961	0	n.d.	17.8
92BS-B	*Ceratodon*	16-Oct-96	0.72±0.15	−34.8±7.9	0.961	69	35	0.3
92BS-C	*Ceratodon*	28-May-96	1.21±0.52	−44.9±18.3	0.844	0	n.d.	19.5
92BS-D	*Ceratodon*	28-May-96		73.0±13.8	0.965	0	n.d.	16.5
92BS-D	*Ceratodon*	5-Jun-96		25.4±5.8	1.000	0	n.d.	27.6
95BS-A	*Ceratodon*	4-Jun-96		state steady		0	n.d.	n.d.
95BS-A	*Ceratodon*	8-Oct-96		6.4±6.2	steady	n.d.	49	7.7
95BS-A	*Ceratodon*	15-Oct-96		1.4±9.1	state*	32	49	0.0
95BS-B	*Ceratodon*	8-Oct-96	0.67±0.08	−28.3±3.1	0.971	n.d.	35	5.4
95BS-B	*Ceratodon*	11-Oct-96		5.1±1.2	0.901	93	36	2.3
95BS-E	*Ceratodon*	30-May-96		state steady		0	n.d.	n.d.
87BS-B	burned moss	29-May-96	1.05±0.08	−34.7±3.5	0.987	0	n.d.	11.8
87BS-C	burned moss	29-May-96	2.97±0.21	−100.0±0.9	0.995	0	n.d.	15.2
87BS-D	burned moss	29-May-96	2.12±0.25	−65.0±11.9	0.959	0	n.d.	21.2
87BS-D	burned moss	4-Jun-96	2.07±0.31	−41.5±8.9	0.958	0	n.d.	18.2
92BS-A	burned moss	22-Jul-94	1.15±0.23	−29.2±7.1	0.927	0	35	23.0
92BS-A	burned moss	4-Aug-94	1.08±0.07	−61.7±8.3	0.991	0	lost	5.9
92BS-A	burned moss	5-Aug-94	1.59±0.12	−64.8±8.9	0.995	0	lost	−0.6
92BS-A	burned moss	5-Aug-94	0.92±0.07	−36.7±5.0	0.988	0	lost	0.9
92BS-A	burned moss	16-Oct-96	1.76±0.32	−38.8±7.2	0.937	69	35	0.1
92BS-E	burned moss	28-May-96	1.78±0.39	−87.6±23.1	0.914	0	n.d.	23.6
92BS-E	burned moss	5-Jun-96		state steady		0	n.d.	27.4
92BS-F	burned moss	29-May-96	0.87±0.06	−33.9±3.4	0.995	0	n.d.	15.2
95BS-C	burned moss	4-Jun-96	1.31±0.18	−32.5±5.8	0.965	0	n.d.	13.8
95BS-C	burned moss	8-Oct-96	0.88±0.08	−29.8±2.9	0.983	n.d.	49	6.2
95BS-C	burned moss	15-Oct-96	0.94±0.13	−27.0±5.2	0.980	32	49	0.0
95BS-D	burned moss	8-Oct-96	1.62±0.08	−60.3±7.7	0.998	n.d.	35	5.7
95BS-D	burned moss	11-Oct-96	2.53±0.41	−70.4±13.3	0.949	93	36	1.1
CBS-A	feather mosses	18-Aug-94	2.82±0.08	−179.0±26.3	0.998	0	45±8	15.0
CBS-A	feather mosses	19-Aug-94	1.27±0.46	−49.3±21.6	0.885	45	45±8	10.8
CBS-A	feather mosses	19-Aug-94	2.33±0.23	−81.8±14.3	0.982	0	45±8	11.6
CBS-A	feather mosses	19-Aug-94	2.18±0.34	−77.1±14.4	0.953	0	45±8	11.7
CBS-A	feather mosses	27-Jul-94	2.33±0.20	−94.9±17.0	0.986	0	22	26.2
CBS-A	feather mosses	28-May-96	1.93±0.14	−49.1±1.5	0.989	0	n.d.	14.3
CBS-A	feather mosses	8-Oct-96	1.02±0.35	−39.4±5.0	0.811	n.d.	19	0.7
CBS-A	feather mosses	15-Oct-96	1.69±0.56	−57.8±2.2	0.900	n.d.	22	0.1
CBS-B	feather mosses	28-May-96	0.95±0.07	−32.5±1.1	0.995	0	n.d.	14.3
CBS-B	feather mosses	2-Jun-96	2.03±0.17	−40.6±4.8	0.980	0	n.d.	3.0
CBS-B	feather mosses	11-Oct-96	2.42±0.39	−70.0±3.8	0.975	21	27	−0.2
CBS-B	feather mosses	15-Oct-96	1.03±0.16	−27.4±4.4	0.954	n.d.	27	0.1

Dep. Vel.: deposition velocity; Light: full spectrum; Moisture: thermally determined of the upper 5 cm of the mineral clay layer; Sur. Temp: surface temperature 1 cm from the top; n.d.: not determined; * initial increase then steady state.

acquired for samples 87BS-5 to 7 collected and measured in 1995. Table 3 gives the composition, dry bulk density, and moisture contents of the cores sampled in 1996. The extremely high porosity of the moss, F- and H-layers, as indicated by the low dry bulk density, suggests that diffusion in these layers is much more rapid than in clay mineral soil layers. Thus, it is not likely that CO uptake was diffusion limited. Soil moisture is another factor influencing CO soil-atmosphere

Table 2. *Average CO deposition velocities determined with static chambers at various sites grouped by soil surface types and temperature ranges*

Surface	Temperature range	average (°C)	Deposition velocity (10^{-2} cm/s)	Numbers of observations	Percent of >10°C
Ceratodon	all	12.2	1.08±0.53	5	
	<10°C	2.6	0.70±0.04	2	52
	>10°C	21.2	1.34±0.55	3	100
burned mosses	all	10.9	1.54±0.64	16	
	<10°C	2.4	1.41±0.57	8	85
	>10°C	18.3	1.66±0.71	8	100
feather mosses	all	9.0	1.83±0.63	12	
	<10°C	0.7	1.64±0.62	5	83
	>10°C	14.8	1.97±0.65	7	100

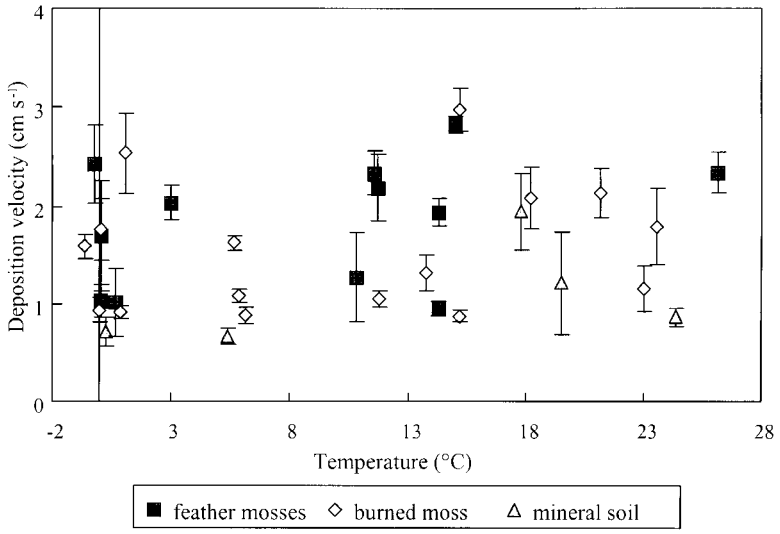

Fig. 1. Temperature dependence of CO deposition velocities for different soil covers as determined with the static chambers (CO emissions determined for some mineral soil sites are not included in this figure).

fluxes. Low soil moisture inhibits microbial activity and high soil moisture inhibits gas exchange between soils and the atmosphere (Conrad and Seiler, 1985b; Funk et al., 1994; Zepp et al., 1996). Thus, both extremes inhibit microbial consumption of atmospheric CO. Moisture contents of three parallel samples were directly measured for comparison to similar samples used in the incubation measurements in order to determine significant changes in soil moisture due to the incubation. In two out of three cases, the moisture content of the parallel samples was lower than in the one used for the incubation measurements, showing that no significant amount of moisture was lost during the incubation measurements. Thus and due to the sufficient moisture content, we concluded that changes in temperature, and not moisture content, were the controlling factor influencing the determined deposition velocities.

Moisture contents were highly variable but always higher than 100% in the organic layers. The highest moisture content of 396% was measured in the living, green feather mosses. The lowest moisture contents of 42% and 55% were deter-

Table 3. *Description and ancillary data for the cores used in the jar experiments*

Site + core	Depth (cm)	Layers	Depth (cm)	Dry bulk density (g/cm^3)	Moisture (%-dm)
CBS-1	0–5	green moss	0–2	0.037	396
		F-layer	2–5		
CBS-2	5–10	F-layer	5–10	0.073	151
CBS-3	10–15	F-layer	10–15	0.161	133
CBS-4	15–20	F-layer	15–15.5	0.449	67
		H-layer	15.5–17		
		clay (balls)	17–20		
92BS-1	0–5	new moss	0–3	0.373	104
		H + charcoal	3–4		
		clay (balls)	4–5		
92BS-2	5–10	clay	5–10	0.822	42
95BS-1	0–5	new moss	0–0.5	0.465	96
		H + charcoal	0.5–3		
		clay (balls)	3–5		
95BS-2	0–5	top charred + F-layer	0–5	0.070	253
95BS-3	5–10	F-layer	5–8	0.126	284
		H-layer	8–10		
95BS-4	10–15	H-layer	10–12	0.541	73
		clay (balls)	12–15		
87BS-1	0–5	top charred + F-layer	0–5	0.037	296
87BS-1C*	0–5			0.061	195
87BS-2	5–10	F-layer	5–10	0.101	264
87BS-2C*	5–10			0.150	313
87BS-3	10–15	H-layer	10–15	0.129	294
87BS-3C*	10–15			0.304	216
87BS-4	15–20	clay (balls)	15–20	0.944	55

dm: dry matter; * control samples to determine changes in soil moisture.

mined for the two pure clay layers and have comparable values to those measured for the static chamber measurements, where the same layer is used. Soil bulk density increased with soil depth from values of 0.04 g cm^{-3} for the top moss layers, through 0.1–0.4 g cm^{-3} for the F- and H-layers, to 0.9 g cm^{-3} for the mineral clay layer.

Table 4 summarises the dark deposition velocities determined from these cores at temperatures ranging from -15°C to 20°C. In all cases consumption of CO was observed. CO consumption generally increased with temperature. Deposition velocities at -13°C and -15°C were only 1–3% of that at 20°C and dramatically increased at 0–1.5°C. At the latter temperature deposition velocities were (43 ± 20)%, and at 4–5°C were (68 ± 15)% of that at 20°C (neglecting 87BS-4). Thus CO soil consumption dramatically increases between -15 and 5°C, and increases more slowly from 5°C to 20°C.

3.3. *CO soil profiles and calculation of thermally produced CO*

Air within the different organic layers down to the mineral soil was sampled with stainless steel tubing and gas-tight glass syringes sealed with a small amount of water. Build-up of CO within these syringes was determined to be 10 ± 6 ppb CO in 6 h when kept at about 0°C in the dark. Since the air samples usually were analysed about 6 h after collection we subtracted 10 ppb CO from the measured CO concentrations at the different depths. The low CO concentrations of 0–30 ppb measured within the soil have an uncertainty of ± 15 ppb. Table 5 summarises soil air CO concen-

Table 4. *Deposition velocities determined by the jar experiment at various temperatures*

Core	Depth (cm)	Top layer	Deposition velocities and standard deviations (10^{-2} cm/s)												
			-15 ± 1°C	▲	%*	0 ± 0.5°C	▲	%*	4 ± 1°C	▲	%*		▲	%*	20 ± 1°C	▲
CBS-1	0–5	green moss	n.d.			1.22 ± 0.19	3	34	2.54 ± 0.32	4	70				3.62 ± 0.04	2
CBS-2	5–10	F-layer	n.d.			0.71 ± 0.04	3	19	2.21 ± 0.14	3	61				3.65 ± 0.53	3
CBS-3	10–15	F-layer	n.d.			1.68 ± 0.09	2	18	5.56 ± 0.43	2	60				9.27 ± 0.71	3
CBS-4	15–20	F-layer	n.d.			4.51 ± 0.40	4	40	8.28 ± 0.45	2	73				11.14 ± 0.78	3
92BS-1	0–5	new moss	0.03 ± 0.002	3	1	2.29 ± 0.72	3	83	2.62 ± 0.30	2	94				2.78 ± 0.20	2
92BS-2	5–10	clay	0.13 ± 0.02	3	3	2.66 ± 0.94	2	56	3.93 ± 0.28	3	82				4.78 ± 0.22	2
95BS-1	0–5	new moss	n.d.			1.07 ± 0.08	2	56	1.35 ± 0.10	2	70				1.92 ± 0.32	2
95BS-2	0–5	F-layer	n.d.			6.58 ± 1.21	3	76	8.09 ± 0.28	2	94				8.62 ± 0.67	4
95BS-3	5–10	F-layer	n.d.			2.59 ± 0.27	2	31	5.23 ± 0.78	3	62				8.41 ± 0.51	2
95BS-4	10–15	H-layer	n.d.			1.13 ± 0.01	2	33	1.69 ± 0.22	3	50				3.42 ± 0.05	2
			-13 ± 1°C			1.5 ± 0.5°C			3 ± 1°C			5 ± 1°C			20 ± 1°C	
87BS-1	0–5	F-layer	0.34 ± 0.04	5	3	3.33 ± 0.28	3	31	9.13 ± 0.26	5	85	6.87 ± 0.06	3	64	10.70 ± 0.66	3
87BS-2	5–10	F-layer	0.18 ± 0.02	5	1	4.19 ± 0.16	3	35	9.23 ± 0.68	3	76	9.21 ± 0.29	4	76	12.10 ± 1.02	5
87BS-3	10–15	H-layer	n.d.			1.43 ± 0.10	5	32	1.91 ± 0.25	3	42	2.35 ± 0.06	2	52	4.53 ± 1.28	4
87BS-4	15–20	clay (balls)	n.d.			0.28 ± 0.03	5	57	0.20 ± 0.03	2	39	0.22 ± 0.14	4	45	0.50 ± 0.11	3
									5 ± 1°C			10–15°C			15–20°C	
87BS-5	0–5	F-layer													10.85 ± 04.73	10
87BS-6	5–10	H + clay													3.01 ± 0.06	4
87BS-7	10–15	clay													0.32 ± 0.03	4
empty									0.006 ± 0.001	2		-0.03	1		-0.039 ± 0.005	2

* % of deposition velocity determined at 20°C; ▲ numbers of observations; n.d. not determined.

Table 5. *CO soil profiles and calculated CO production*

Site	Depth in moss (cm)	Date	Temp. (°C)	CO (ppb)	CO Dep. (10^{-2} cm s^{-1})	CO-Prod. (10^{9} molec. cm^{-2} s^{-1})
CBS	5	11-Oct.-96	0.2	44	0.71	8.4
	10	11-Oct.-96	0.4	27	1.68	12.2
	15	11-Oct.-96	1.3	29	4.51	35.0
	10	8-Oct.-96	3.0	14	5.56	20.7
	20	8-Oct.-96	4.2	4	n.d.	
	22.5	8-Oct.-96	4.2	0	n.d.	
87BS	−5 (in snow)	12-Oct.-96	0.0	103		
	0	12-Oct.-96	0.1	34[a]	3.33	3.0[a]
	2	12-Oct.-96	0.2	9	3.33	8.1
	2	12-Oct.-96	0.2	5	3.33	4.5
	5	12-Oct.-96	1.7	22	4.19	24.6
	10	12-Oct.-96	2.0	4	1.43	1.5
	16.5	12-Oct.-96	2.5	14	0.35	1.3
	5	15-Oct.-96	1.7	19	4.19	21.3
95BS	5	11-Oct.-96	1.0	25	2.59	17.3
	10	11-Oct.-96	2.3	31	1.13	9.3
	15	11-Oct.-96	3.4	25	1.69	11.2
	20	11-Oct.-96	4.0	24	n.d.	
87BS[b]	0–5 (incubation) litter, coniferous	27-Sept.-95	15–20	20	10.84	55.7
	woodland[c]		10			≈10.0
			20			≈45.0
Andalusia[d]		10-Sept.-82	30.0	51	≈1.10	12.3
			0.0	3	≈0.75	6.7

[a] Not at steady state; [b] equilibrium CO mixing ratio determined with the incubation method; [c] data from Moxley and Smith (1998); [d] 30°C values from Conrad & Seiler, 1985b, 0°C values extrapolated from Conrad & Seiler, 1985; n.d.: not determined.

trations and lists depth, temperature, and date of sampling. No significant trend in CO data with depth can be identified. On 12 October 1996 when about 10 cm of snow covered the soil, CO could be measured in the snow and directly at the soil-snow interface. In this case, the CO concentration decreased to 2 cm in the soil and then remained fairly constant at greater depths. The lack of a trend for the days when no snow covered the soils indicates that CO concentrations at depths greater than 5 cm in soils are not significantly influenced by diffusion of atmospheric CO into the soil. This finding is supported by the fact that in nearly all cases, deposition velocities in the top 5 cm determined by the incubation method exceeded or equalled the deposition velocities determined by the static chamber technique (see Subsections 3.1. and 3.2.).

Thus measured CO concentrations below 5 cm in the soil can be assumed to be at a steady state that is determined by thermal formation and microbial consumption of CO. At this steady state, or compensation concentration as defined by Conrad and Seiler (1985b), the gross production rate (p) equals the gross consumption rate (c), so that the production rate can be derived from

$$p = c = m_e d \tag{1}$$

where m_e is the CO mixing ratio at equilibrium and d the deposition velocity. To calculate the CO production rates, the measured CO mixing ratios and deposition velocities determined by the

incubation study for the corresponding depth were used. The production rates given in Table 5 may be looked at as upper limits since the measured equilibrium CO concentrations may be too high due to contamination by ambient air that was present in the tubing despite flushing.

CO production as given in Table 5 ranges from 1.3 to $35 \cdot 10^9$ molec. CO cm^{-2} s^{-1} at the given temperatures of 0–4°C.

4. Discussion

4.1. Temperature dependence of CO deposition velocities

No significant temperature dependence of dark deposition velocities was determined on site with the static chambers (Table 2, Fig. 1). Still, for all three soil surface groups, average deposition velocities were somewhat lower for soil surface temperatures below 10°C compared to those for above 10°C (Table 2). This agrees with the findings of the incubation measurements where a strong temperature dependence of deposition velocities was observed.

No temperature induced change from CO sink to source for the temperature range studied here (−15°C to 20°C incubation, −0.6°C to 27.6°C static chambers) is apparent from this data set. Still, the only dark CO flux measurement at a burned moss site showing a steady-state concentration and no sink activity is the one with the highest soil surface temperature of 27.4°C. For Venezuelan savanna soils (2.1 ± 0.5C %-dm), Scharffe et al. (1990) determined a change from CO sink to source at soil surface temperatures around 30°C with ambient CO concentrations between 220–280 ppb. Zepp et al. (1996) measured only CO emissions from South African savanna soils for surface temperatures ranging from 17°C to 43°C most likely due to drought-inhibited microbial activity. For an Andalusian soil with an organic carbon content of 0.5%-C of dry mass, CO production equalled microbial CO oxidation at surface temperatures of approximately 40°C (ambient CO 150–180 ppb; Conrad and Seiler, 1985b).

Previous studies (Scharffe et al., 1990; Conrad and Seiler, 1985b) found microbial consumption of CO to be nearly independent of temperatures from 20–40°C. This study shows a significant increase in CO consumption in the temperature range from −15° to 5°C and a slight increase from 5°C to 20°C. The soil temperature range from 20°C upwards is most significant in tropical and subtropical regions, whereas the temperature range investigated in this study is representative for temperate to boreal ecosystems.

4.2. Soil cover and depth dependence of net CO fluxes

Average CO deposition velocities determined in dark or low-light conditions with the static chamber and grouped by soil cover types indicate significantly higher dark or low-light velocities for soils covered with either burned or green feather mosses compared to sites that were burned down to the mineral soil (Table 2). Of all static chamber measurements, only sites that had been burned down to the mineral soil showed significant dark CO source activity. At site 92BS-D, high soil moisture (inhibit gas transport, anaerobic conditions) in addition to soil temperature may be the significant factors that contributed to the source activity (Funk et al., 1994; Moxley and Smith, 1998). Higher soil moisture most likely only influenced those sites that were burned down to the mineral soil and/or are covered only with a thin layer of new moss. Moss covers at the other sites were normally deeper than 10 cm and we rarely noticed standing water underneath the moss. In the case of two studies, 95BS-A and 95BS-B, where surface temperature ranged between 0°C and 7.7°C and soil moisture 36%-dm and 49%-dm, respectively, the incident light of 32 W m^{-2} and 93 W m^{-2} may have been the determining factor for the source activity.

Only a slight, statistically insignificant decrease in sink activity was determined for the burned moss compared to the undisturbed green feather moss sites (Table 2). These results indicate that microbial consumption of CO is higher in the moss layers compared to the mineral clay and that no significant difference concerning CO consumption exists between living, green feather moss and burned moss.

Clear differences between soil covers can be identified with the incubation measurements at 20°C (Table 4). The lowest deposition velocities were determined for the new moss (*Ceratodon*) and pure clay cores 87BS-4 and -7. This finding agrees

well with the low deposition velocities determined with the static chambers at sites that burned down to the mineral soil. The exceptionally high deposition velocity determined for the pure clay core 92BS-2 can not be explained. The F-layers, especially those close to the H-layer, were the most active layers; deposition velocities generally increase with depth down to the H-layer and then decrease with deposition velocities generally lower for clay layers than for green moss or H-layers. Fluxes determined from cores of the 87BS site that were sampled and measured in 1995 (87BS-5 to 7) compared well with those determined from similar layers in 1996 (87BS-1 to 4; Table 4). At the unburned feather moss site (CBS), CO consumption rates increased with depth. There, the highest deposition velocity was measured for the core (CBS-4), which included only a thin F-layer (0.5 cm), followed by a 1.5 cm H-layer, and 3 cm of mineral clay. The deposition velocity for CBS-4 is comparable to those measured for the top 10 cm of the burned moss at the 87BS and 95BS sites.

Differences between the sites are less pronounced at 0–1.5°C, although the trends are the same as observed at 20°C. Again, while CO consumption decreases with depth at the burned moss sites, it increases at the living, green feather moss site. No definite explanation of this difference between the living green moss and burned moss sites can be given. It may be that CO-consuming microbes are more active in the F- and H-layer than in the green moss.

It is interesting to compare the two new moss cores. Deposition velocities were always higher for the *Ceratodon* moss core from 92BS compared to that from the 95BS site. The new moss was 3 cm thick at 92BS-1 but only 0.5 cm thick at 95BS-1. Thus the higher deposition velocity for the former may be explained by the thicker new moss layer. Secondly, it seems that deposition velocities of the new moss are less dependent on temperature than the feather moss F- and H-layers neglecting core 95BS-2.

4.3. *Thermally produced CO*

In nearly all cases, deposition velocities obtained from cores of the top 5 cm by the incubation method exceed or equal the deposition velocities determined by the static chamber technique at equivalent temperatures. Only in one case (CBS-B, 11-Oct.-96, Table 1) does the deposition velocity determined with the static chamber exceed that of the incubation method. This result indicates that only the top 5 cm of soil determines dark CO deposition fluxes. Thus soil CO profiles below 5 cm should only be influenced by thermal production and microbial oxidation of CO. This observation is strengthened by the absence of a trend for CO concentrations at depths greater than 5 cm (Table 5). This fact was used to calculate thermal CO production (see 3.3) at the various sites. Table 5 summarises the determined CO production and consumption rates.

Conrad and Seiler (1985b) determined thermal production rates of $(1.5–115)\cdot10^9$ molec. CO $cm^{-2}\,s^{-1}$ at 30°C. Their deposition velocities and rates of thermal formation of CO determined from Andalusian soils (Spain) for 30°C and extrapolated to 0°C are given in Table 5 for comparison. It is interesting to note that the range given by Conrad and Seiler (1985b) for 30°C is similar to ours for temperatures around 2°C despite the strong correlation between thermal CO formation and temperature that they observed. Based on the relationship between CO production and temperature, our production rates appear too high. However, Conrad and Seiler saw a strong linear correlation between CO production rates and organic carbon contents of soils as well. The lowest production rate of $1.45\cdot10^9$ molec. CO $cm^{-2}\,s^{-1}$ was determined for soils with 0.1% dry weight organic carbon content, and $115\cdot10^9$ molec. CO $cm^{-2}\,s^{-1}$ for soils with 3.9% dry weight organic carbon content. Thus production rates of $(1.3–35)\cdot10^9$ molec. $cm^{-2}\,s^{-1}$ at 2°C for the F- and H-layer in the upland Canadian forest with carbon contents around 45% dry weight may be reasonable. This is stressed by CO production rates determined for coniferous litter (C-content >40% dry weight) by Moxley and Smith (1998). They calculated CO production rates of about 10 and $40\cdot10^9$ molec. $cm^{-2}\,s^{-1}$ at 10°C and 20°C, respectively. The single determination of thermal CO production at 87BS at 15–20°C (by incubation) shows an increase by a factor of 5–13 compared to the values at 2°C from the field profiles. By comparison, a factor of 18 increase of thermal CO production for a temperature increase from 0°C to 20°C is derived from the Arrhenius equa-

tion of thermal CO formation as given by Conrad and Seiler (1985b) for Andalusian soils.

5. Conclusions

Static chamber measurements indicated significantly higher dark or low-light CO deposition velocities for soils that were covered by either burned or living, green feather mosses [$(1.54 \pm 0.64) \cdot 10^{-2}$ cm s^{-1}; $(1.83 \pm 0.63) \cdot 10^{-2}$ cm s^{-1}] than for sites that had burned down to the mineral soil [$(1.08 \pm 0.53) \cdot 10^{-2}$ cm s^{-1}, excluding net CO emission]. Incubation measurements of CO deposition velocities confirmed that the highest consumption rates occurred in the moss, particularly in the F-layer. CO deposition velocities showed the highest rate of increase from -15° to 5°C and only a moderate increase from 5°C to 20°C. On average, about 70% of the sink activity observed at 20°C was already achieved at 4–5°C. Similarly, the results of the static chamber study indicated a slight, though not statistically significant increase in deposition velocities from below 10°C to above 10°C.

In nearly all cases, deposition velocities determined for cores from the upper 5 cm by the incubation technique were equal to or greater than those determined in the field with the static chambers. This along with the low CO mixing ratios within the moss and the absence of a trend of the CO mixing ratios with depth, indicates that only the upper most 5 centimetres determine the dark CO soil-atmosphere exchange at these sites. Interestingly, the upper-most 5 centimetres of these soils are also exposed to the greatest ranges in temperature (and probably moisture) differences and are most affected by fire as well.

Thermal CO formation at various depths (C-content $\approx$45% dry weight) was calculated to be (1.3 to 35)$\cdot 10^9$ molec. CO cm^{-2} s^{-1} at temperatures around 0°C. Moxley and Smith (1998) determined thermal CO production of litter from coniferous woodland (C-content >40% dry weight) to be about 10 and $45 \cdot 10^9$ molec. CO cm^{-2} s^{-1} at 10°C and 20°C, respectively. Conrad and Seiler (1985b) measured $12.3 \cdot 10^9$ molec. CO cm^{-2} s^{-1} at 30°C for soils with organic carbon contents of 0.1–3.9% dry weight. This latter lower production rate of CO can thus be explained by the lower soil organic carbon content.

The temperature and moisture range chosen for this study of upland Canadian forest soils is representative of nearly the entire 6 snow-free months of this area. Dark deposition velocities determined in this study are representative of low-light and night-time conditions.

We conclude that fires that take place during a dry period and burn moss down to the mineral soils have a significant effect on CO consumption by boreal upland forest soils. Fires that only burn the top of the moss layer do not significantly reduce CO consumption of boreal soils. Fire frequency and intensity in boreal forests are likely to increase significantly if global warming occurs (Kasischke et al., 1995). This could lead to an increase in area that is burned down to the bare soil and thus may significantly decrease the CO consumption capability of boreal forests. Still, the results do not totally explain the conversion of boreal forests from CO sinks to sources by fires (Zepp et al., 1998). The combination of higher incident light and soil temperatures, due to the removal of forest canopy, and lower CO consumption rates may explain this conversion from sink to source.

6. Acknowledgements

We thank two anonymous referees for their thorough and helpful comments. T. Kuhlbusch acknowledge financial support of the National Research Council for these studies.

REFERENCES

Alperin, M. J. and Reeburgh, W. 1985. Inhibition experiments on anaerobic methane oxidation. *Applied and Environm. Microbiol.* **50**, 940–945.

Beke, G. J., Veldhuis, H. and Thie, J. 1973. *Bio-physical land inventory of the Churchill-Nelson rivers study area north-central Manitoba.* Canada-Manitoba Soil Survey, University of Manitoba, Winnipeg, 57, 110.

Bessie, W. C., and Johnson, E. A. 1995. The relative importance of fuels and weather on fire behaviour in subalpine forests. *Ecology* **76**, 747–762.

Conrad, R. 1995. Soil microbial processes and the cycling of atmospheric trace gases. *Phil. Trans. R. Soc. Lond.* **A 351**, 219–230.

Conrad, R. and Seiler, W. 1980. Role of microorganisms

in the consumption and production of atmospheric carbon monoxide by soil. *Appl. Environm. Microbiol.* **40**, 437–445.

Conrad, R. and Seiler, W. 1985a. Characteristics of abiological carbon monoxide formation from soil organic matter, humic acids, and phenolic compounds. *Env. Sci. & Tech.* **19**, 1165–1169.

Conrad, R. and Seiler, W. 1985b. Influence of temperature, moisture, and organic carbon on the flux of H_2 and CO between soil and atmosphere: Field studies in subtropical regions. *J. Geophys. Res.* **90**, 5699–5709.

Funk, D. W., Pullman, E. R., Peterson, K. M., Crill, P. M., and Billings, W. D. 1994. Influence of water table on carbon dioxide, carbon monoxide, and methane fluxes from taiga bog microcosms. *Global Biogeochem. Cycles* **8**, 271–278.

Kasischke, E. S., Christensen, N. L. Jr. and Stocks, B. J. 1995. Fire, global warming, and the carbon balance of boreal forests. *Ecological Applications* **5**, 437–451.

Moxley, J. M. and Smith, K. A. 1998. Factors affecting utilisation of atmospheric CO by soils. *Soil. Biol. Biochem.* **30**, 65–79.

Scharffe, D., Hao, W. M., Donoso, L., Crutzen, P. J. and Sanhueza E. 1990. Soil fluxes and atmospheric concentrations of CO and CH_4 in the northern part of the Guayana Shield, Venezuela. *J. Geophys. Res.* **95**, 22 475–22 480.

Tarr, M. A., Miller, W. L. and Zepp, R. G. 1995. Direct carbon monoxide production from plant matter. *J. Geophys. Res.* **100**, 11 403–11 413.

Troxler, R. F. 1972. Synthesis of bile pigments in plants: Formation of carbon monoxide and phycocyanobilin in wild-type and mutant strains of the alga *Cyanidium caldarium*. *Biochemistry* **11**, 4235–4242.

Van Wagner, C. E. 1983. Fire behaviour in northern conifer forests and shrublands. In: *The rôle of fire in the northern circumpolar ecosystems* (eds. W. Wein and D. A. MacLean). SCOPE 18, John Wiley & Sons, New York, 65–80.

Wilks, S. S. 1959. Carbon monoxide in green plants. *Science* **129**, 964–966.

Zepp, R. G., Miller, W. L., Burke, R. A., Parsons, D. A. B. and Scholes, M. C., 1996. Effects of moisture and burning on soil-atmosphere exchange of trace carbon gases in southern African savanna. *J. Geophys. Res.* **101**, 23 699–23 706.

Zepp, R. G., Miller, W. L., Tarr, M. A., Burke, R. A. and Stocks, B. J., 1998. Soil-atmosphere fluxes of carbon monoxide during early stages of post-fire succession in upland Canadian boreal forests. *J. Geophys. Res.* **102**, 29 301–29 312.